I&EC research
Industrial & Engineering Chemistry Research

Article

pubs.acs.org/IECR

Hansen Solubility Parameters for Octahedral Oligomeric Silsesquioxanes

Andrew J. Guenthner,*[,†] Kevin R. Lamison,[‡] Lisa M. Lubin,[‡] Timothy S. Haddad,[‡] and Joseph M. Mabry[†]

[†]Propulsion Directorate, Air Force Research Laboratory, Edwards AFB, California 93524, United States

[‡]ERC Incorporated, Air Force Research Laboratory, Edwards AFB, California 93524, United States

Supporting Information

ABSTRACT: The Hansen Solubility Parameters (HSP) for several polyhedral oligomeric silsesquioxane (POSS) compounds were successfully determined, demonstrating the applicability of the HSP approach for selected types of organic−inorganic compounds. As commonly practiced with organic polymers, a set of simple "pass/fail" tests for complete solubility at a fixed concentration (100 mg/mL) was conducted for an array of five octameric POSS compounds, octa(phenethyl), octa(styrenyl), octa(*iso*butyl), octakis(hexafluoro*iso*butyl), and (1-naphthyl)heptaphenyl), and 45 test solvents. Group contributions for the octameric POSS cage were determined using three different approaches, which produced similar results. The best cage contribution estimate for the dispersive, polar, and hydrogen-bonding components δ_D, δ_P, and δ_H of the total solubility parameter was determined to be $\delta_D = 22$ $(J/cc)^{1/2}$, $\delta_P = 19$ $(J/cc)^{1/2}$, and $\delta_H = 15$ $(J/cc)^{1/2}$, with an estimated uncertainty of approximately 5 $(J/cc)^{1/2}$. The utility of the HSP approach was demonstrated by successfully identifying mixtures of poor solvents that provided significantly enhanced solubility for octa(*iso*butyl) POSS, and by successfully estimating the HSP of octakis(trifluoropropyl) POSS from group contributions derived solely from aromatic POSS compounds.

1. INTRODUCTION

Over the past few decades, Hansen Solubility Parameters (HSP) have achieved a high level of prominence in the coatings industry as a practical tool for estimating a variety of thermodynamic and transport properties in polymer systems.[1−4] An advantage of the HSP approach over the simpler one-component Hildebrand solubility parameter theory is that the HSP approach enables the identification of mixtures of nonsolvents that, when combined in the proper ratio, become good solvents for difficult to dissolve polymers.[5] The adoption of the HSP approach to the more general problem of finding sets of polymers and/or small-molecule fluids that display desired thermodynamic interaction characteristics, whether favorable or unfavorable, has saved countless hours of trial and error in gas separation membranes,[6] drug delivery,[7−9] and nanocomposite[10−15] applications. It is, therefore, virtually certain that successful efforts aimed at expanding the range of applicability of Hansen Solubility Parameters will generate numerous very substantial positive impacts across a wide variety of industries.

Polyhedral oligomeric silsesquioxanes (POSS)[16] are a family of inorganic/organic core/shell nanostructures possessing molecular weight values on the order of 1000 g/mol, in which the core consists of a silsesquioxane cage with the formula $(SiO_{1.5})_n$, where n is generally between 8 and 14. The shell consists of n organic functional groups originating at each Si atom on a cage vertex. Cages are generally categorized according to the bonding type and number of silicon atoms that comprise each vertex. The functionality may vary from one organic group to another, although the most commonly used compounds feature octameric cages with identical, simple functional groups.

Since their commercialization in the late 1990s, POSS compounds have found a large variety of uses, particularly as modifiers for polymers and inorganic fillers in the medical,[17] aerospace,[18] and electronics industries,[19] where they serve as processing aids for high-temperature thermoplastics, dispersion and compatibilization agents, and thermal and electrical insulation enhancers. The inorganic core is both mechanically robust, resistant to oxidation, and thermally stable, and the ability to synthesize a variety of peripheral groups makes the tailoring of properties fairly straightforward. Despite the many applications for POSS compounds that involve thermodynamic compatibility and mixing, there have been few systematic comparative attempts to quantify POSS solubility in common organic solvents.[20,21]

More significant effort, however, has been devoted to exploring the solubility of inert POSS compounds in polymers.[16,19] There have been numerous reports of good compatibility between certain POSS compounds and selected polymers, e.g., octakis(2-phenylethyl), referred to as octa(phenethyl), POSS and either polystyrene[22] or polyvinyl chloride.[23] However, in many cases, the reported solubility of POSS compounds in polymers of interest is quite limited. Therefore, there is a clear need for a rational approach to determine the solubility and thermodynamic interactions of POSS compounds with both solvents and polymers.

Despite the obvious need, there has been only a small amount of published work to date on the solubility parameters of POSS compounds. Recent work reported by the Morgan

Received: March 22, 2012
Revised: June 26, 2012
Accepted: August 28, 2012
Published: August 28, 2012

group[24−26] has focused on determination of the Hildebrand solubility parameters of POSS compounds with partial success in predicting polymer compatibility. Other recent work by Lim et al.[27,28] has shown that calculation of the HSP for the peripheral arms of POSS compounds (ignoring the cage entirely) provides limited comparative insight into polymer compatibility as well. Further work along these lines has also very recently been reported by Dintcheva et al.[29] Most recently, Milliman, Boris, and Schirladi[30] have determined the Hansen Solubility Parameters for a few POSS compounds, and shown, importantly, that the Hansen approach offers greatly improved predictive capabilities for POSS/polymer miscibility.

In general, the Hansen Solubility Parameter approach has been limited to purely organic compounds, with only a few investigations performed for inorganic groups[31,32] (mainly in the context of nanoparticles or surfaces[13−15,33−37]), or for organic/inorganic polymers, such as polysiloxanes[38−40] and polyphosphazines.[41] The size and even shape of POSS molecules, however, would not be expected to preclude the determination of HSP because the HSP approach has been successfully applied to compounds such as fullerenes,[12,42] asphaltenes,[43−46] and bitumen[47,48] that are intermediates between small molecules and polymer chains. Though for nanoparticles in general, one would expect the solubility parameters to reflect the surface, rather than bulk composition, for POSS compounds, the central cage is at least partially accessible to surrounding molecules, and the overall issue of solvent accessibility is similar to those encountered for many types of polymers. In short, given the many benefits that will accrue from successful application of HSP to POSS compounds, the subject is worth considerable further investigation.

Herein we report the results of our efforts to determine Hansen Solubility Parameters for selected POSS compounds. We found that, for an initial group of five POSS compounds, simple solubility testing of the type carried out for polymers was adequate for the determination of the HSP values. We further found that the consistency of the results was of the same quality encountered for most polymer systems, and that there appeared to be no fundamental disadvantage associated with POSS compounds as a group. Additional analysis of these HSP values allowed us to investigate the possibility of assigning a group contribution to the octameric cage, where we determined that, although a reasonably consistent set of parameters could be obtained for many compounds, the issue of cage accessibility may complicate matters more than in a typical polymer. Our results represent an important extension of HSP in the realm of inorganic/organic materials, a significant but logical step forward that is certain to bring substantial benefits to the ever growing array of applications in which POSS compounds are featured prominently.

2. EXPERIMENTAL SECTION

2.1. Materials. Octa(phenethyl) POSS, octa(styrenyl) POSS, octakis(hexafluoro*iso*butyl) POSS, (1-naphthyl)-heptaphenyl POSS, and octakis(trifluoropropyl) POSS were synthesized at AFRL. Octa(*iso*butyl) POSS was obtained from Hybrid Plastics (Hattiesburg, MS). The chemical structure of these compounds is given in Figure 1. A large amount of data is available for the octa(*iso*butyl) compound,[16] with limited data available for the octa(phenethyl),[22,23,49−55] octa(styrenyl),[54,56] octakis(hexafluoro*iso*butyl),[57] and, more recently, the (1-naphthyl)heptaphenyl[21] compounds. The set of 45 solvents

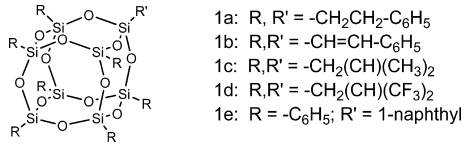

Figure 1. Chemical structure of POSS compounds for which HSP were determined.

used in the study were obtained from a variety of commercial sources. Most were of technical grade, and all were used in as-received condition. All are listed in Supporting Information (SI) Section S2.

2.2. Test Procedures. The experimental procedures reported herein closely follow those outlined by Hansen.[1] For each of the tests reported herein, 50 mg of the POSS compound was placed in a clean 5-mL glass vial along with 0.5 mL of the selected solvent. The tightly closed vials were then stirred for 2 min and checked for dissolution. When complete dissolution did not occur, the vials were allowed to stand for up to 1 h. The tests were then rated as follows: "Pass" indicated complete dissolution within two minutes; "Pass −" indicated complete dissolution within 1 h but not within 2 min (in these cases, most of the solute dissolved initially and extra time was required to achieve complete dissolution, an indication of near saturation given the low molecular weight of the POSS compounds); "Fail +" indicated that significant but incomplete dissolution occurred; "Fail" indicated that little or no dissolution was observed. Note that, unless otherwise noted, "Pass −" was treated as "Pass" and "Fail +" was treated as "Fail" for the purposes of analysis, thus all "good" solvent systems were given at least 1 h to achieve complete dissolution.

2.3. Analysis Procedures. The primary goal of the analysis for a given POSS compound was to provide the best available estimate of the dispersive (δ_D), polar (δ_P), and hydrogen bonding (δ_H) components of the Hansen Solubility Parameter. The basis for these procedures has been described in detail by Hansen,[1] and involves a commonly used geometrical interpretation of the data. As a result, many terms that refer to geometric characteristics are often encountered in describing Hansen Solubility Parameter data. To aid those readers who may be less familiar with these terms, a glossary has been included in SI Section S1. In addition to the typical best estimate of solubility parameters and the "radius of interaction" (R_0) that defines the expected boundary in "HSP space" between "good" and "poor" solvents, we also developed some simple methods that provide an indication of the uncertainty in the HSP values reported (since HSP data do not obey simple normal or binomial distribution functions, definitive methods for characterizing uncertainty are unavailable, but we believe it is important to at least provide some indication of uncertainty when reporting results.)

The basic approach was to maximize the goodness of fit of the data set to the "sphere of solubility" based on the pass/fail ratings (here denoted as "test$_i$" and the associated HSP ($\delta_{D\text{-}S,i}$, $\delta_{P-S,i}$, $\delta_{H-S,i}$) of each solvent tested. Namely, for each instance i, a characteristic distance R_a was defined such that

$$R_{a,i} = 4*(\delta_{D-POSS} - \delta_{D-S,i})^2 + (\delta_{P-POSS} - \delta_{P-S,i})^2 + (\delta_{H-POSS} - \delta_{H-S,i})^2 \quad (1)$$

with the expected criteria being

dx.doi.org/10.1021/ie300767p | Ind. Eng. Chem. Res. 2012, 51, 12282−12293

If $R_{a,i} < R_0$, then test_i = "Pass". Otherwise, test_i = "Fail"

in which $\delta_{\text{D-POSS}}$, $\delta_{\text{P-POSS}}$, $\delta_{\text{H-POSS}}$, and R_0 were adjustable parameters. The goodness of fit was determined by means of a χ^2 test, using the total fraction of tests evaluated as "Pass" and the total fraction of solvents for which $R_{a,i} < R_0$ to determine the distribution of expected occurrences. The procedure described above was the computational equivalent of attempting to identify the central coordinates and radius of a sphere that included all solvents with a "pass" rating but excluded all solvents with a "fail" rating, in a Cartesian space with axes given by 2 δ_D, δ_P, and δ_H.

To locate the optimal values of $\delta_{\text{D-POSS}}$, $\delta_{\text{P-POSS}}$, $\delta_{\text{H-POSS}}$, and R_0, a brute force method based on an iteratively refined search space was employed. In the first iteration, $\delta_{\text{D-POSS}}$ was varied from 15 to 20 in increments of 0.5, while $\delta_{\text{P-POSS}}$ and $\delta_{\text{H-POSS}}$ were varied from 0 to 10 in increments of 1, while R_0 was varied from 0 to 20 in increments of 0.25. The initial range represented a compromise between comprehensiveness and the need to minimize computation time, and was based on the range of the HSP noted for solvents with a rating of "pass". For every possible combination of the four parameters given the ranges and increments listed above, the χ^2 parameter was then calculated and the absolute maximum was recorded. For the second iteration, the search grid was centered on the point having maximum χ^2 (with the lowest value of all other parameters used to break ties) found in the previous iteration, with the increments reduced to 0.4 for $\delta_{\text{D-POSS}}$, and 0.8 for $\delta_{\text{P-POSS}}$ and $\delta_{\text{H-POSS}}$, while the increment was maintained at 0.25 for R_0. (These values were chosen to provide conveniently divisible intervals for subsequent iterations while enabling the search space to be expanded well beyond the originally chosen boundaries if necessary.) The process was repeated two additional times, centering the grid as described previously and reducing the increment for $\delta_{\text{D-POSS}}$, $\delta_{\text{P-POSS}}$, and $\delta_{\text{H-POSS}}$ by a factor of 4 each time, while maintaining the increment for R_0. The method provided a final search resolution of 0.025 for $\delta_{\text{D-POSS}}$, 0.05 for $\delta_{\text{P-POSS}}$ and $\delta_{\text{H-POSS}}$, and 0.25 for R_0. Note that the finer spacing for $\delta_{\text{D-POSS}}$ was used to compensate for the factor of 4 in the Hansen expression (effectively, the parameter 2 $\delta_{\text{D-POSS}}$ was used as a dimension along with $\delta_{\text{P-POSS}}$, and $\delta_{\text{H-POSS}}$ in a uniform Cartesian search grid that shrank with each iteration until the optimal center coordinates were identified).

Due to the highly nonlinear nature of the optimization process, many possible locations in "HSP space" bounded by an irregular and even noncontiguous region can be of equal or nearly equal goodness of fit, thus it is important to obtain some estimate of uncertainty. To address this issue, we again employed a brute force method, calculating the χ^2 value for all combinations of $\delta_{\text{D-POSS}}$, $\delta_{\text{P-POSS}}$, $\delta_{\text{H-POSS}}$, and R_0 with increments of 0.05, 0.1, 0.1, and 0.25, respectively, around the optimal point identified in the final search iteration with a span of 11 increments for $\delta_{\text{D-POSS}}$, $\delta_{\text{P-POSS}}$, and $\delta_{\text{H-POSS}}$ and 41 increments for R_0. We considered χ^2 values that differed from the previously determined optimum by less than one to be representative of equivalent goodness of fit. This practice, based on a related suggestion by E. von Meerwaal of the University of Akron, was found to work quite well in this situation. The values of every combination of $\delta_{\text{D-POSS}}$, $\delta_{\text{P-POSS}}$, and $\delta_{\text{H-POSS}}$ for which at least one value of R_0 enabled the condition for equivalent goodness of fit to be met were logged. If any of these coordinates fell on the boundary of the search region, the increments of $\delta_{\text{D-POSS}}$, $\delta_{\text{P-POSS}}$, and $\delta_{\text{H-POSS}}$ were increased in linear steps of 100% (i.e., they were first doubled from their original values, then tripled from their original values, etc.), and the entire process repeated, until no coordinates on the boundary of the search region met the goodness of fit criteria. We then calculated the centroid and radii of gyration (in each dimension) of the set of all coordinates that met the goodness of fit criteria, using the centroid for the finally determined values of the HSP for the given POSS compound. The R_0 values from the list of all coordinate combinations that met the goodness of fit criteria were averaged and reported as the final R_0 value for the POSS compound. The radii of gyration were then reported as indicators of the "characteristic uncertainty" of the measurement.

3. RESULTS AND DISCUSSION

3.1. General Overview. Figures 2−6 depict the outcomes of the solvent testing for the octa(phenethyl) (Figure 2),

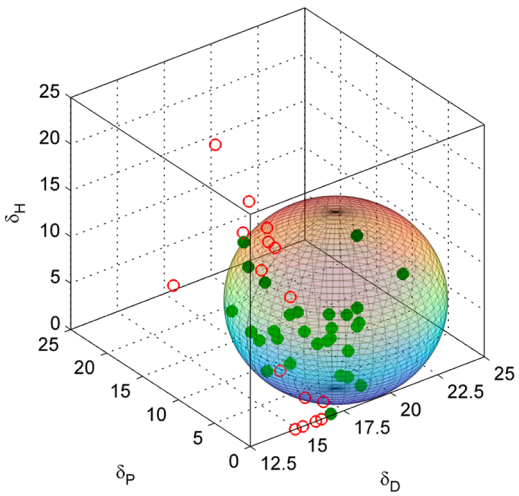

Figure 2. Results of solubility testing for octa(phenethyl) POSS. Filled symbols indicate solvents with a rating of "pass" (complete solubility at 100 mg/mL), while open symbols indicate solvents with a rating of "fail". The "sphere of solubility" that best describes the data (based on maximizing χ^2) is also shown.

octa(styrenyl) (Figure 3), octa(*iso*butyl) (Figure 4), octakis-(hexafluoro*iso*butyl) (Figure 5), and (1-naphthyl)heptaphenyl (Figure 6) POSS compounds. In each of these figures, the axes represent the HSP with the scaling suggested by Hansen,[1] with δ_D stretched by a factor of 2. The filled symbols represent the HSP of solvents that rated "pass", while the unfilled symbols reflect the solvents that rated "fail". The spherical object represents the predicted "pass/fail" boundary, based on the calculated HSP for the individual POSS compound (the center coordinates of the sphere) and the calculated value of the "radius of interaction" R_0. Numerical values of the calculated HSP, R_0, characteristic uncertainties (see Experimental Section for details), and data on the overall solubility have been provided in Table 1, as well as the number of failed predictions based on the relative energy difference (RED) concept,[1] in which the RED is defined as the ratio of the distance in "HSP space" between the coordinates of the POSS compound and the solvent to R_0, with "good" solvents expected when RED < 1 and "poor" solvents expected for RED > 1. Note that additional views of the data shown in Figures 2−6, with data points labeled by solvent identifier, are provided in SI Figures S2−S6.

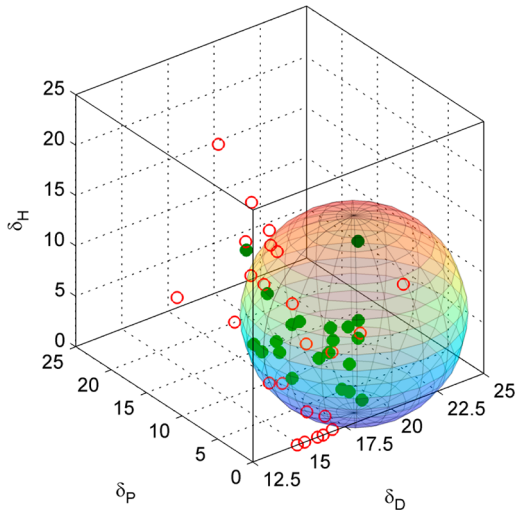

Figure 3. Results of solubility testing for octa(styrenyl) POSS, with data displayed as in Figure 2.

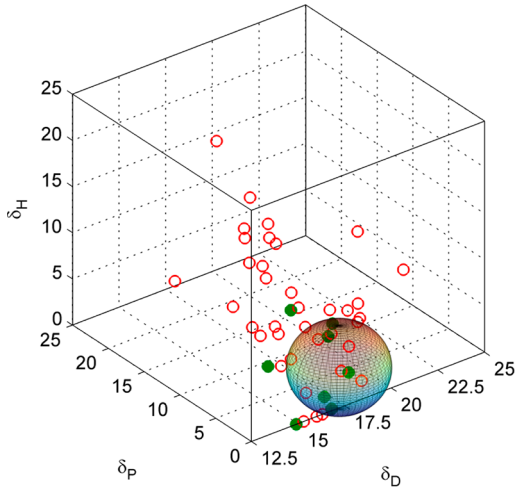

Figure 4. Results of solubility testing for octa(*iso*butyl) POSS, with data displayed as in Figure 2.

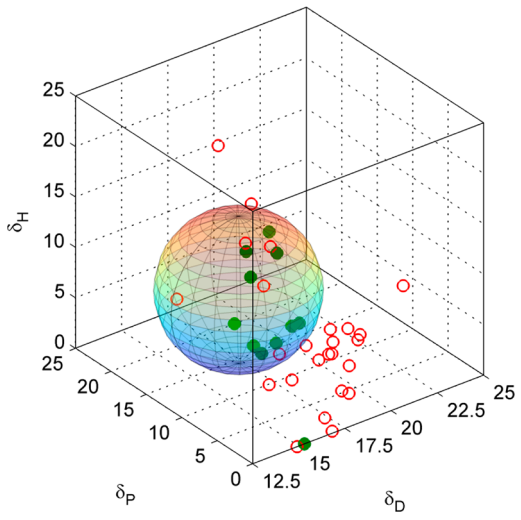

Figure 5. Results of solubility testing for octakis(hexafluoro*iso*butyl) POSS, with data displayed as in Figure 2.

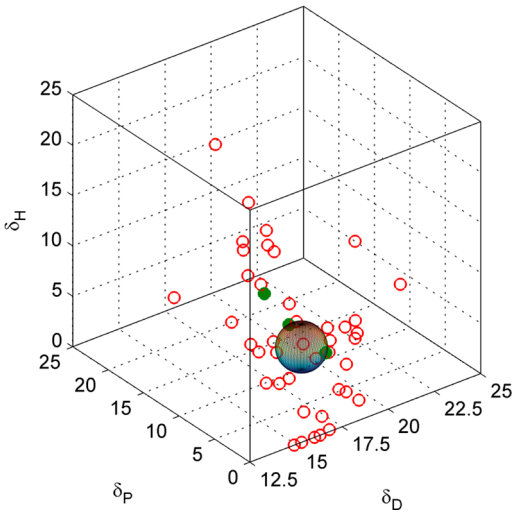

Figure 6. Results of solubility testing for (1-naphthyl)heptaphenyl POSS, with data displayed as in Figure 2.

Perhaps the most important general result that can be appreciated from examination of Figures 2−6 is the level of success of the HSP approach for the POSS compounds. In general, the best fit predictions result in errors (counting both anomalous good and anomalous poor solvents) of only approximately 25% as often as they successfully identify good solvents, whereas assigning otherwise randomly chosen guesses based only on the proportion of solvents rated "pass" for a particular compound results in about 2.5 errors for every good solvent successfully identified. In other words, the use of HSP for POSS compounds results in about a 90% reduction in time lost to trial and error.

3.2. HSP of Individual POSS Compounds. Of the POSS compounds examined, octa(phenethyl) POSS (Figure 2) proved to be the most generally soluble, achieving a rating of "pass" in 29 out of the 45 solvents tested (specific ratings for each solvent are provided in SI Tables S1−S3). All but two of the passing solvents, and none of the failing solvents, lay inside a sphere of radius 9.8 centered at (δ_D, δ_P, δ_H) = (19.9, 7.4, 6.3). The two exceptions were cyclohexane and diethyl ether, which were only slightly outside the sphere. The uncertainty in the determined HSP values could be traced to a lack of nonsolvents with a suitably high δ_D value, which results in less than optimal constraint on the location of the sphere of solubility. Such a lack of optimal constraint is a fairly common issue when HSP determinations are performed.[1]

Two additional attempts to generate an octa(phenethyl) POSS solubility data set that was more easily constrained were made. First, the set of solubility tests was repeated using a concentration of 200 mg/mL, rather than 100 mg/mL, with the intent of generating fewer passing solvents and shrinking the radius of interaction. Although the number of passing solvents was reduced to 19, this approach was unsuccessful because the solvents with the highest δ_D still passed. By disproportionately eliminating solvents that helped to constrain the sphere, the uncertainties were in fact made worse. (Data for this and other "Supplemental" tests is provided in Table 2). Second, an additional two solvents and ten solvent mixtures (listed in SI Table S3) were chosen based on their location in "uncharted" regions of HSP space near the probable boundary of the sphere of solubility and tested at 100 mg/mL. The results were then combined with those from the original 45 solvents. The second

dx.doi.org/10.1021/ie300767p | *Ind. Eng. Chem. Res.* 2012, 51, 12282−12293

Table 1. Estimated HSP and Selected Related Characteristics of Octameric POSS Compounds (Standard Analysis)

name (code)	δ_D centroid	δ_D R_G[a]	δ_P centroid	δ_P R_G	δ_H centroid	δ_H R_G	R_0	no. good/no. tested	no. anomalies
octa(phenethyl) (PE-1)	19.9	0.4	7.4	0.5	6.3	0.6	9.8	29/45	2
octa(styrenyl) (ST-1)	20.2	0.7	5.8	0.8	6.6	0.7	9.8	21/45	5
octa(*iso*butyl) (IB-1)	18.0	0.1	2.1	0.2	2.7	0.3	4.3	8/45	6
octakis(hexafluoro*iso*butyl) (HF-1)	15.3	0.8	9.3	0.9	11.0	0.6	7.3	10/36	2
(1-naphthyl)heptaphenyl (NP-1)	16.9	0.1	4.0	0.2	6.3	0.2	2.5	3/45	1

[a] R_G = radius of gyration, a measure of the uncertainty.

Table 2. Estimated HSP and Selected Related Characteristics of Octameric POSS Compounds (Supplemental Analysis)

analysis (code)	δ_D centroid	δ_D R_G	δ_P centroid	δ_P R_G	δ_H centroid	δ_H R_G	R_0	no. good/no. tested	no. anomalies
octa(phenethyl) @ 200 mg/mL (PE-A1)	21.6	0.5	6.2	0.2	9.9	0.4	11.8	19/45	2
octa(phenethyl) with additional solvents and mixtures (PE-A2)	19.7	0.3	8.0	0.2	5.6	0.4	9.6	35/57	3
(1-naphthyl)heptaphenyl @ 50 mg/mL (NP-A1)	16.9	0.1	4.0	0.2	6.3	0.2	2.5	3/45	1
(1-naphthyl)hepta-phenyl with "fail +" considered equal to "pass" (NP-A2)	18.1	0.2	8.6	0.3	6.7	0.1	4.3	7/45	2

procedure was modestly effective at further constraining the sphere of solubility. The results, as seen in Table 2, were changed little in terms of actual HSP coordinates. However, the uncertainties were reduced.

The solubility of octa(styrenyl) POSS, a more rigid analog of octa(phenethyl) POSS, was predicted only modestly less accurately by the "spherical rule", with five exceptions (all nonsolvents within the sphere) out of 45 solvents, and with three of the exceptions exhibiting partial solubility. Though octa(styrenyl) POSS was somewhat less soluble overall (21 passing solvents) compared to octa(phenethyl) POSS, the R_0 values for octa(styrenyl) and octa(phenethyl) POSS were equivalent. The octa(styrenyl) POSS had a slightly higher δ_D value than octa(phenethyl) POSS, meaning that its calculated HSP also were made more uncertain by lack of constraints.

Though known for its good polymer compatibility characteristics,[16] which likely result from its relatively low melting point rather than necessarily from good intrinsic solubility, octa(*iso*butyl) POSS (Figure 4) exhibited a significantly smaller radius of interaction than either octa(phenethyl) or octa(styrenyl) POSS. Though well-constrained, the solubility envelope appeared less well-defined, with six exceptions (three of each type) found. Given that only eight solvents passed (with eight also found inside the sphere), the odds that a solvent having sufficiently similar HSP to octa(*iso*butyl) POSS was, in fact, a good solvent were just over 60%. On the other hand, good solvents for octa(*iso*butyl) POSS were found at RED values (the distance to the center of the sphere divided by the radius of interaction) of 1.6. Interestingly, the anomalous poor solvents (benzene, xylenes, and phenyl acetylene) were all small aromatic hydrocarbons, while toluene was soluble at 100 mg/mL). The anomalous good solvents were *n*-hexane, diethyl ether, and tetrahydrofuran. While the predictive power for the HSP approach was less effective for octa(*iso*butyl) POSS than for any other compound in this study, it was still on par with test results from many organic polymers. It should be noted that for octa(*iso*butyl)POSS, there were 12 instances in which partial solubility was noted, compared to typically only 3−5 instances for other POSS compounds. Thus, the solubility behavior of octa(*iso*butyl)POSS may be quantitatively more complex compared to other POSS compounds, and may be better understood using more sophisticated approaches.

To further explore similar POSS compounds, testing was undertaken with 36 solvent candidates on octakis(hexafluoro*iso*butyl) POSS (Figure 5), a member of the class of compounds known as "fluoro POSS" that have played a key role in realizing superoleophobicity on rough surfaces.[57−59] The octakis(hexafluoro*iso*butyl) POSS was in general more soluble than octa(*iso*butyl) POSS, having a larger radius of interaction. There were also just two exceptions to the "spherical rule", *iso*propanol (an anomalous poor solvent lying just inside the boundary of the sphere, note that 1-propanol and 1-butanol were good solvents and within the sphere), and *n*-heptane (an anomalous good solvent).

Finally, a highly aromatic POSS compound was also examined, (1-naphthyl)heptaphenyl POSS (Figure 6). Although most aromatic POSS compounds are very poorly soluble, the asymmetric substitution pattern appears to enable at least limited solubility.[21] A total of three good solvents enabled a rudimentary estimate of the HSP for the compound, with a small radius of interaction and just one exception to the "spherical rule", albeit a crucial one: 1-methyl-2-pyrrolidone proved to be a good solvent despite having an RED value of 3.4. With only three good solvents, it is difficult to justify ignoring this anomaly on the basis of only two other data points.

In an effort to clarify the HSP for this compound, attempts were made to identify more "good" solvents to improve the robustness of the analysis. First, the nonsolvents were all retested at a lower concentration of 50 mg/mL to try and broaden the criteria for inclusion of "good" solvents. Unfortunately, in every case for which the aromatic POSS compound failed to dissolve at 100 mg/mL, it also failed to dissolve completely at 50 mg/mL. However, in addition to the three "good" solvents (chloroform, tetrahydrofuran, and 1-methyl-2-pyrrolidone), there were four solvents in these tests that received the "fail +" rating, meaning that partial solubility was noted. Although less quantitative than using solubility at a specific concentration such as 100 mg/mL to differentiate between "pass" and "fail" ratings, adding these four solvents to the list of "good" solvents allowed for a more robust calculation of the HSP, with the results shown in Table 2. In this case, no poor solvents lay within the sphere of solubility, and only two good solvents (chloroform and diphenyl ether) were found outside of the sphere, in both cases by a short distance.

3.3. Estimation of Group Contribution Parameters for Octameric POSS Cages. Having identified HSP for five POSS compounds, it is reasonable to consider whether or not a

Table 3. Calculated Arm Group Cohesive Energies (J/cc) for POSS Compounds

	best available analog group			Beerbower GC			Stefanis GC		
arm type	E_D	E_P	E_H	E_D	E_P	E_H	E_D	E_P	E_H
-phenethyl x 8	312000	350	1930	331000	1670	1670	320000	1850	10
-styrenyl x 8	320000	930	15500	311000	2880	13700	290000	2440	100
-*iso*butyl x 8	154000	0	0	142000	0	0	159000	2360	210
-hexafluoro-*iso*butyl x 8	178000	0[a]	0	90400	67000	0	227000	10500	2490
-(1-naphthyl) + -phenyl x 7	212000	120	2650	273000	1810	1810	246000	2550	210

[a]The value for analog groups is unavailable and therefore set arbitrarily to zero.

systematic pattern exists with respect to the HSP of the peripheral groups. If a systematic pattern does exist, then it should be possible to identify a "group contribution" for the octameric POSS cage at the core of the five compounds studied. With such a "group contribution" in hand, it would then be possible to calculate estimated HSP for any octameric POSS compound. (Other methods based on more sophisticated computational techniques[60−66] might also be useful in estimating the HSP for POSS compounds. However, a group contribution approach would be highly valuable due to its simplicity.) It should be noted, however, that with HSP data available for only a very few compounds, any such group contribution estimates will, of necessity, be of a rough, preliminary nature.

To determine whether a meaningful group contribution exists, one may formally divide the cohesive energy of the POSS compounds into two parts, one arising from the cage and one arising from the peripheral arms, or

$$E_{i,\mathrm{POSS}} = E_{i,\mathrm{cage}} + \sum_{n}^{j=1} E_{i,j\mathrm{th-arm}} \tag{2}$$

in which E_i represents the ith cohesive energy component (dispersive, polar, or hydrogen bonding) for a system comprising the central cage and n peripheral organic groups (arms), not all of which are necessarily identical. This formal division is the simplest method that allows for modeling of a wide variety of POSS compounds, and the division of a complex structure into a set of simpler substructures is an almost universal feature of group contribution approaches to calculation of solubility parameters as illustrated by the method of Constantinou.[67] If values for $E_{i,j\mathrm{th\text{-}arm}}$ can be calculated through existing group contribution methods, then the total component cohesive energy densities for the POSS cage may be used to generate an independent estimate of all $E_{i,\mathrm{cage}}$ for every POSS compound measured. If a volume contribution for the cage can be determined, then component solubility parameters for the cage may also be estimated. By examining the consistency of the values of $E_{i,\mathrm{cage}}$ (or the cage solubility parameters) derived from different compounds, a sense may be developed as to whether a single meaningful parameter exists, as well as a sense of what limitations are inherent to the approach.

The estimation of the geometric parameters of POSS cages for the purposes of providing group contribution estimates has not appeared in published work that we are aware of, and is an important prerequisite for determination of solubility parameters. For interested readers, we have provided a detailed account of how the relevant geometric parameters were computed in SI Section S3. The key result for solubility parameter determinations was that a molar volume of 134 cc/mol was assigned to the POSS cage.

Table 3 shows estimates for the cohesive energy components of the arms, based on three theoretical methods, the best available analog group method described in Appendix A (for which a direct calculation of the energy components is employed), the Beerbower group contribution method as reported by Hansen[1] (again, for which a direct calculation of the energy components is available), and a more recent method described by Stefanis.[68] Unlike the other two methods, the Stefanis group contribution involves a calculation of group HSP, these are then multiplied by the experimental arm volume to obtain the dispersive, polar, and hydrogen bonding cohesive energy components, E_D, E_P, and E_H, respectively. The Stefanis method is available without modification for all groups needed. However, the Beerbower method is not directly applicable to the 1-naphthyl group or the fluorocarbon groups for all components. To make use of the Beerbower method, two assumptions are employed. First, the cohesive energy for the naphthyl group is calculated by scaling the values for phenyl groups by the number of carbons (10 for naphthyl as opposed to 6 for phenyl); second, the $-CF_3$ group contribution for the polar component is calculated by taking the listed value for the total energy and subtracting the values of the other two components (which are listed as zero), even though the contribution of the polar component is listed as "?". As described in Appendix A, the best available analog group method can only generate an estimate for the dispersive component of the cohesive energy of the hexafluoro*iso*butyl group. Although a negligible contribution from hydrogen bonding to the cohesive energy density of this group represents a reasonable assumption, we have herein also used a negligible contribution from the polar component for lack of a more suitable alternative.

From Table 3, it can be seen that the agreement among the different methods differs according to which component of cohesive energy density is being considered. For the dispersive component, the agreement is best for the phenethyl, styrenyl, and *iso*butyl arms, fair for the 1-naphthyl-heptaphenlyl combination, and poor for the hexafluoro*iso*butyl arms. This is the same pattern of agreement seen for estimates of geometrical parameters, and reflects the relative maturity of group contribution methods for the various groups involved. For the polar component, the differences among methods are relatively small in absolute terms for all but the hexafluoro*iso*butyl group, for which the methods provide widely diverging estimates. For the hydrogen bonding component, the analog group and Beerbower methods agree well with one another, while the Stefanis method provides somewhat different estimates.

To obtain estimated group contribution HSP values for the POSS cages, the total cohesive energies for the compounds as a whole were calculated based on the experimental solubility parameters and molar volumes, subtracted from the calculated

cohesive energy values for the arms, and then divided by the estimated cage volume (134 cc/mol) before raising to the 0.5 power. Tables of the HSP component solubility parameter estimates for the POSS cage based on each of the three computational methods (Beerbower, Stefanis, and analog group for cohesive energy) are shown in SI Section S4, and include a measure of the sensitivity of the calculated HSP group contributions to expected input errors. Table 4 summarizes the results, based on the analog group method for computing arm contributions and the more reliable alternative analyses of experimental data for octa(phenethyl) POSS and 1-naphthyl-heptaphenyl POSS.

Table 4. Calculated Group Contribution from POSS Cage Based on HSP Analysis of POSS Compounds Best Available Analog Group Contributions for Arms

compound used to calculate cage component	calculated cage δ_D	calculated cage δ_P	calculated cage δ_H
octa(phenethylPOSS[a]	22.9	21.6	14.7
octa(styrenyl)POSS	23.1	15.3	14.0
octa(*iso*butyl)POSS	25.8	5.0	6.4
octa(hexafluoro*iso*butyl)POSS	14.2	23.8	28.1
1-naphthyl-heptaphenyl POSS[a]	20.2	21.1	15.9

[a]Using alternative analysis −A2 (extra solvents for octa(phenethyl)-POSS, and "fail+" counted as "pass" for 1-naphthylheptaphenyl POSS).

As expected, extracting a meaningful cage contribution from the data on octakis(hexafluoro*iso*butyl) POSS was the most problematic. The main issue, however, appears to be not the experimental data, but rather the inability to determine a reasonable estimate of the cohesive energy components for the arms, particularly for the dispersive and polar components. For the polar and hydrogen bonding components, the inferred cage cohesive energy values are considerably higher than those derived from measurements of the other POSS compounds. One possible explanation would be a strong electronic interaction unique to POSS compounds with fluorinated arms, as suggested by X-ray data,[58] between the cage and the fluorine atoms on the arms, at least some of which must approach the cage closely due to the particular geometry of the arms.

Another issue apparent from Table 4 is that the polar and hydrogen bonding components of the cage cohesive energy inferred from measurements of octa(*iso*butyl) POSS are much lower than those derived from the other POSS cages. Among the POSS compounds analyzed, octa(*iso*butyl) POSS conformed the least to the "spherical rule". However, the derived cage contributions appear relatively insensitive to the characteristic uncertainties in the experimental measurement. Instead, it appears as though the apparent strongly polar and hydrogen bonding character of the cage is screened by the *iso*butyl arms. Note, however, that simply ignoring the cage and assigning HSP values based only on the cohesive energy and volume (calculated from the best available analog group method) of the peripheral groups, which leads to (δ_D, δ_P, δ_H) = (15.8, 0, 0) for octa(*iso*butyl)POSS, results in a decrease of almost 70% in the χ^2 statistic even in the best case (R_0 = 2.25), thus, screening of the POSS cage, if responsible for the observed HSP behavior, is likely only partial. Such a partial screening effect could result from the more oblate shape of the *iso*butyl arms in comparison to the other POSS types. In fact, it does seem to be the case, based on the limited data set generated, that POSS compounds with more prolate arms (such as phenethyl, styrenyl, and (1-napthyl)heptaphenyl) provided more consistent cage contributions. Such a "prolate arm" configuration should involve less direct interaction between the cage and the arms, and thus ought to be more amenable to analysis by additive group contributions.

Despite all of the difficulties, it does appear that, at least for the prolate arm types, a "consensus" value for the cage contributions is available. As with all group contribution methods, there is a considerable amount of uncertainty. However, in many cases, group contribution methods are utilized to provide rough estimates. In these cases, the values provided by averaging the octa(phenethyl) (alternate case −A2, which appears to be slightly more precise), octa(styrenyl), and (1-napthyl)heptaphenyl alternative −A2) would seem to be provide the best estimate. For the best available analog group method, the averages are δ_D = 22 $(J/cm)^{1/2}$, δ_P = 19 $(J/cm)^{1/2}$, and δ_H = 15 $(J/cm)^{1/2}$, or, in terms of cohesive energy components, E_D = 65000 J/mol, E_P = 48000 J/mol, and E_H = 30000 J/mol. Although a characteristic uncertainty is not readily assigned to these values, based on the data in Table 4, most of the values for the three compounds lie within about 5 $(J/cm)^{1/2}$ of these averages. As with any group contribution method, HSP data for many additional POSS compounds will be needed in order to transform the rough estimate provide above into a highly reliable predictive tool.

3.4. Tests of the HSP and Group Contribution Approaches for POSS Compounds. To truly evaluate the usefulness of the HSP approach, as well as the group contribution approach to estimating HSP, for POSS compounds, two specific tests of predictive power were performed. For HSP in general, one of the most useful predictive features is the ability to identify mixtures of nonsolvents that can serve as a good solvent. Thus, guided by the calculated HSP values, we sought to identify a mixture of two poor solvents that displayed anomalously good solubility for a POSS compound. For this demonstration, we chose octa(*iso*butyl) POSS because its location on the HSP diagram and its relatively small radius of interaction provide for many possible nonsolvent combinations, and because it showed a large number of exceptions to the "spherical rule", hence it serves as a fairly stringent test of the theory. 1,4-Dioxane and *n*-heptane, both of which are poor solvents for octa(*iso*butyl) POSS, were chosen for the experiment. In Figure 7, quantitative solubility data for octa(*iso*butyl) POSS in mixtures of 1,4-dioxane and *n*-heptane are presented as a function of composition. These two

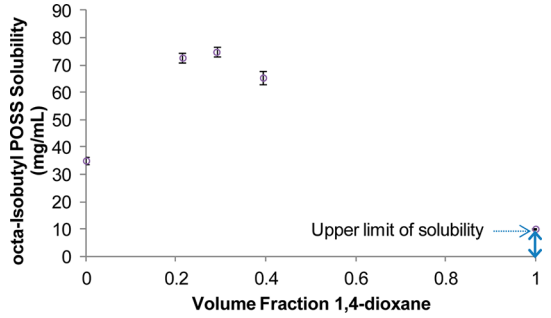

Figure 7. Solubility of octa(*iso*butyl) POSS at 20 °C as a function of 1,4-dioxane fraction in a mixed solvent system containing *n*-heptane and 1,4-dioxane.

nonsolvents were the first fully miscible pair we tested (*n*-hexane and 1,1,2,2-tetrabromoethane, as well as 1-decene and quinoline, which we also attempted to test, were not fully miscible with one another).

As is clearly evident in Figure 7, a significant improvement in solubility is obtained when *n*-hexane and 1,4-dioxane are utilized as a mixed solvent system for octa(*iso*butyl) POSS. Although, strictly speaking, the most soluble mixtures fall somewhat short of the "pass" threshold of 100 mg/mL, despite the fact that they lie just within the sphere of interaction on the HSP diagram, they are more than twice as soluble as *n*-hexane alone and about four times as soluble as a simple rule of mixtures would predict. Moreover, the most soluble mixtures, containing 25−30 vol% 1,4-dioxane, are reasonably close in composition to the value (about 45 vol% 1,4-dioxane) that corresponds to the minimum RED for the mixed solvent system based on the measured HSP values for octa(*iso*butyl) POSS. Thus, at a qualitative level, the predictions of HSP theory were confirmed for octa(*iso*butyl) POSS.

To test the group contribution approach, we again chose a stringent challenge for the theory. The compound octakis(trifluoropropyl) POSS[69] has been previously reported in studies of liquid repellent surfaces,[70] and is potentially useful as an additive to fluoropolymers. Therefore, knowledge of its HSP would have many practical benefits. Currently, however, the pure compound (containing only octameric cages) is available in extremely limited quantities, making direct measurement of its HSP using a full set of solvents impractical. Although fluoroalkyl groups pose a challenge for many group contribution approaches, general estimates of both volume and cohesive energy are still possible. The trifluoropropyl arms are also of a small, prolate shape, so cage effects should be distinguishable and the group contribution approach should be applicable. Table 5 lists the calculated volumetric, cohesive energy, and HSP data for octakis(trifluoropropyl) POSS and its components based on the three theoretical approaches outlined earlier, with details of the best available analog group method provided in Appendix A for cohesive energies and SI Section S3.3 for volume. For the Stefanis approach, calculation of the cohesive energy components requires a separate model for calculation of the molar volume. In this case, the best available analog group method was chosen, since, in cases where data on analogous compounds are readily available, it tended to predict volumes more accurately (and, unlike the case for hexafluoro*iso*butyl groups, such data are readily available for trifluoropropyl groups). For the HSP calculations, the best available analog group method is based on the best available analog group volume estimates, the Beerbower method is based on the Beerbower volume estimates, and the Stefanis method does not require a volume estimate.

As for the radius of interaction, there is no explicit predictive method available. However, based on the data in Tables 1 and 2, it can be seen that the radius of interaction generally increases with the size and flexibility of the arms. Also, comparing *iso*butyl and hexafluoro*iso*butyl arms, it appears that fluorination leads to an increase in the radius of interaction. The trifluoropropyl group is somewhat smaller than the *iso*butyl group, but contains limited fluorinated groups as well. If these two factors approximately counteract each other, one would expect a radius of interaction for the octakis(trifluoropropyl) POSS that is similar to the octa(*iso*butyl) POSS, or about 4.3.

To compare these predictions to experimental data, octakis(trifluoropropyl) POSS was dissolved in 20 test solvents. Using the predicted solubility parameters and the predicted radius of interaction, RED values for each solvent were assigned and compared against the same "pass/fail" criteria (100 mg/mL solubility at room temperature) used for the other compounds. The results are tabulated in SI Section S5. Also, based on this limited data set, a maximization of χ^2 according to the method described in the Experimental Section was undertaken, and yielded estimates of δ_D = 16.9 $(J/cc)^{1/2}$, δ_P = 9.1 $(J/cc)^{1/2}$, δ_H = 8.9 $(J/cc)^{1/2}$, and R_0 = 4.5 with indicated uncertainties of 0.3−0.5 $(J/cc)^{1/2}$, five good solvents and no exceptions to the "spherical rule". Given the limited data set and the many uncertainties inherent in group contribution methods, the predicted values (which involved no adjustable parameters) agreed quite well with the experimental data. These results reinforce the earlier results that suggest the HSP approach is well-suited to POSS cages, and that group contributions for POSS cages can be utilized on at least certain types of POSS. They also illustrate that the quality of available group contribution values for the peripheral arms on POSS cages

Table 5. Predicted Molar Volume, Cohesive Energy, and HSP for Octakis(Trifluoropropyl) POSS

model/parameter	best available analog group	Beerbower	Constantinou/Stefanis
molar volume (cc/mol)			
each trifluoropropyl arm	79	79	n/a
cage	134	134	134
octakis(trifluoropropyl) POSS	766	766	n/a
cohesive energy (J/mol)			
model/parameter	best available analog group	Beerbower	Constantinou/Stefanis
dispersive component			
each trifluoropropyl arm	13200	11300	19100
cage	65000	65000	65000
octakis(trifluoropropyl) POSS	171000	156000	217000
polar component			
each trifluoropropyl arm	3940	4190	1490
cage	48000	48000	48000
octakis(trifluoropropyl) POSS	80000	81000	60000
hydrogen bonding component			
each trifluoropropyl arm	0	0	80
cage	30000	30000	30000
octakis(trifluoropropyl) POSS	30000	30000	31000
Hansen Solubility Parameters $(J/cc)^{1/2}$			
model/parameter	best available analog group	Beerbower	Constantinou/Stefanis
dispersive component			
each trifluoropropyl arm	12.9	12.0	17.0
cage	22	22	22
octakis(trifluoropropyl) POSS	14.9	14.3	18.2
polar component			
each trifluoropropyl arm	7.0	7.3	4.8
cage	19	19	19
octakis(trifluoropropyl) POSS	10.2	10.3	9.5
hydrogen bonding component			
each trifluoropropyl arm	0	0	1.1
cage	15	15	15
octakis(trifluoropropyl) POSS	6.3	6.3	6.9

dx.doi.org/10.1021/ie300767p | *Ind. Eng. Chem. Res.* 2012, 51, 12282−12293

represents a major consideration when developing group contributions for the cage.

Although the present work has shown the utility of the HSP approach in understanding the solubility behavior of POSS compounds in small molecule solvents, a significantly greater payoff will be achieved if these results can be extended to POSS/polymer blends, as the very recent work published by the Schiraldi group illustrates.[30] In considering the HSP approach to predicting the miscibility of POSS compounds with polymers, there remain several important, yet unanswered questions. First, in the present work, as when determining HSP for polymers, the radius of interaction is considered a characteristic of the POSS compound rather than the solvent. For POSS/polymer blends, however, it is unclear which radius is more appropriate—that of the polymer, that of the POSS compound (which does vary significantly), or some combination of both. Second, a widely reported benefit to blending POSS compounds into polymers is the creation of free volume, which presumably results from an inability of polymer chains to penetrate the complex geometry of the POSS nanostructure. In polymer/solvent and POSS/solvent systems, the relatively small size and comparatively simple geometry of the solvent molecules allows them to "fit in" to complex geometries and mitigate these effects, but in POSS/polymer systems, the "intermeshing" of nanostructures, or lack thereof, may play a significant role in controlling miscibility. The HSP approach is not well-suited to capturing these potentially important effects. The present work, however, by demonstrating that HSP values are a meaningful representation of cohesive energy in POSS compounds (and potentially for silicate nanostructures in general), are compatible with group contribution approaches, and have significant predictive power, effectively lays the groundwork for future investigations of these remaining issues.

4. CONCLUSIONS

Hansen Solubility Parameters (HSP) for five different polyhedral oligomeric silsesquioxane (POSS) compounds have been successfully determined, demonstrating that the HSP approach developed primarily for organic compounds and polymers may be extended to at least limited types of organic–inorganic compounds. In general, the relative energy difference (i.e., "spherical rule") provided good to excellent predictive power, with somewhat less reliable predictions for octa(*iso*butyl) POSS at 100 mg/mL. Though a consistent analysis procedure was employed for all compounds, it was found that alternative analyses provided superior estimates of HSP when either the number of good solvents was very low, or when too few poor solvents were available to properly constrain the boundary of the sphere of solubility. Group contributions for the octameric POSS cage were determined using three different approaches, which gave similar results, with the best estimate being δ_D = 22 $(J/cc)^{1/2}$, δ_p = 19 $(J/cc)^{1/2}$, and δ_H = 15 $(J/cc)^{1/2}$, with an estimated uncertainty of approximately 5 $(J/cc)^{1/2}$. A major constraint in deriving and using these estimates was the ability of the various group contribution methods to correctly model the contributions from the peripheral arm groups. The utility of the HSP approach was demonstrated by successfully identifying mixtures of poor solvents that provided significantly enhanced solubility for octa(*iso*butyl) POSS, and by successfully estimating the HSP of octakis(trifluoropropyl) POSS from group contributions derived solely from aromatic POSS compounds.

APPENDIX A

Description of the Best Available Analog Group Method for Estimates of Cohesive Energy Components

Note that the specific assumptions, data sources, and calculations for these estimates have been provided in SI Section S4. What follows is a description of the method itself and its application to the specific compounds studied. The method is simple enough that in most cases, the means by which it may be adapted to other compounds of interest should be evident to those with even a basic knowledge of group contribution methods.

The foundation of many successful group contribution methods for estimation of the molar cohesive energy is the successful assumption that it is directly proportional to the number of functional groups with only a small dependence on how those groups are arranged. For instance, the cohesive energy of the compound biphenyl is assumed to be exactly twice that of benzene in numerous group contribution methods that have proven reliable over many years. Therefore, attachment to a POSS cage can be assumed to have only a small effect on the cohesive energy of a particular arm, and thus the cohesive energy of a given arm may be assumed to equal that of its free molecule analog (e.g., the cohesive energy of a phenethyl arm is assumed to equal that of ethylbenzene). Moreover, for the purposes of the method, it is assumed that the distribution of cohesive energy components also does not change significantly with attachment to a POSS cage.

For phenethyl, styrenyl, naphthyl, and phenyl arms, experimentally derived cohesive energy components for the analogous free molecules are widely available, and for computational purposes, the values provided by Hansen[1] were used. For *iso*butyl arms, the cohesive energy components of *iso*butane were needed. In general, aliphatic hydrocarbons are assumed to have no polar or hydrogen bonding components of cohesive energy. Therefore, for *iso*butane, the total cohesive energy was determined by the thermodynamic relation

$$E = \Delta H_{vap} - RT \tag{A-1}$$

where ΔH_{vap} is the molar heat of vaporization at 298 K, the experimental value of which was readily available, R is the universal gas constant, and T is the absolute temperature. The total cohesive energy was then assumed to equal the dispersive component of the cohesive energy, with the other components being zero.

For the hexafluoro*iso*butyl arm, experimental data on the analogous compound, hexafluoro*iso*butylene, were not readily available. However, the components of cohesive energy for hexafluoro*iso*butylene were estimated in the tables provided by Hansen.[1] In this case, comparative heat of vaporization data for *iso*butylene and *iso*butane were also used to estimate the effect of hydrogenation on the dispersive component of the cohesive energy, and the difference was applied as a correction to the value for hexafluoro*iso*butylene to estimate the value for hexafluoro*iso*butane. Because the dispersive energy of organic compounds is often calculated on the basis of the total cohesive energy of the hydrocarbon homo-morph for non-fluorinated compounds, and because the difference in saturation involves a non-fluorinated portion of the molecule, the aforementioned procedure appears reasonable for the dispersive component of the cohesive energy. For the polar and hydrogen bonding components, a quick scan of cohesive energy data tables indicated that no obvious simple correction exists for

comparing saturated and unsaturated compounds, so no estimation of these components was attempted for the hexafluoro*iso*butyl arm. Rather, they were simply assumed to equal zero. Note that the hydrogen bonding component of the cohesive energy for many fluorocarbons is generally assumed to equal zero in many group contribution methods as well, leaving only the polar component in question. Because fluorination of aliphatic hydrocarbons affects both dispersive and polar components of cohesive energy, the hydrocarbon homomorph does not provide a reliable means of estimating only the dispersive component.

For the trifluoropropyl arm, cohesive energy components for 1,1,1-trifluoropropane were not readily available, though an experimental value for ΔH_{vap} at 298 K was found. The closest analog with component data estimated by Hansen is 1,1,1-trifluoroethane, although based on the NIST thermodynamic tables for 1,1,1-trifluoroethane, it appears the molar volume and solubility parameters listed are valid only at 174 K. The same NIST thermodynamic tables, however, allow for the calculation of ΔH_{vap} at 298 K. Although the distribution of cohesive energy among its components could vary somewhat with temperature, for simplicity it was assumed that the distribution remained unchanged, and the component values were simply scaled to the corrected total. Having estimated cohesive energy components for 1,1,1-trifluoroethane, it was assumed that the presence of an additional methylene group would add mainly to the dispersive component of the cohesive energy. Therefore, the polar and hydrogen bonding components were taken to be those of 1,1,1-trifluoroethane, while the difference between their sum and the experimentally determined total based on ΔH_{vap} at 298 K was assigned to the dispersive component.

These examples illustrate the need for judicious intuition that makes the best available analog group method less attractive in some respects. In addition, it should be noted that in some cases the values for the analog compounds themselves are merely better established estimates. Therefore, while the best available analog group method has the advantage of a more direct connection to experimental data for common compounds, in cases such as fluorocarbons, where other group contribution approaches have limited success, this method also suffers from significant limitations.

■ ASSOCIATED CONTENT

Supporting Information

Additional text, tables, and graphics as mentioned in the text. This material is available free of charge via the Internet at http://pubs.acs.org.

■ AUTHOR INFORMATION

Corresponding Author

*E-mail: andrew.guenthner@edwards.af.mil.

Notes

The authors declare no competing financial interest.

■ ACKNOWLEDGMENTS

Financial support for this work from the Air Force Office of Scientific Research and the Air Force Research Laboratory, Space and Missile Propulsion Division, is gratefully acknowledged. We thank Mr. Patrick Ruth and Ms. Amanda Wheaton of ERC Inc. for gas pycnometry, and Dr. Sean Ramirez of ERC Inc. for X-ray crystallographic data in support of this work. The octa(phenethyl) and octa(styrenyl) POSS used in this study were prepared by Dr. Rusty Blanski of AFRL, and the 1-napthylheptaphenyl POSS used in this study was prepared by Mr. Brian Moore of AFRL.

■ REFERENCES

(1) Hansen, C. M. *Hansen Solubility Parameters: A User's Handbook*, 2nd ed.; CRC Press: Boca Raton, FL, 2007.

(2) Vink, P.; Bots, T. L. Formulation parameters influencing self-stratification of coatings. *Prog. Org. Coat.* **1996**, *28*, 173−181.

(3) Hansen, C. M. 50 Years with solubility parameters - past and future. *Prog. Org. Coat.* **2004**, *51*, 77−84.

(4) Hansen, C. M. Cohesion parameters for surfaces, pigments, and fillers. *JOCCA-Surf. Coat. Int.* **1997**, *80*, 386−&.

(5) Hansen, C. M. The three-dimensional solubility parameter – key to paint component affinities I. *J. Paint Technol.* **1967**, *39*, 104−117.

(6) Dong, G. X.; Li, H. Y.; Chen, V. Factors affect defect-free Matrimid (R) hollow fiber gas separation performance in natural gas purification. *J. Membr. Sci.* **2010**, *353*, 17−27.

(7) Hellsten, S.; Qu, H. Y.; Louhi-Kultanen, M. Screening of Binary Solvent Mixtures and Solvate Formation of Indomethacin. *Chem. Eng. Technol.* **2011**, *34*, 1667−1674.

(8) Dwan'Isa, J. P. L.; Rouxhet, L.; Preat, V.; Brewster, M. E.; Arien, A. Prediction of drug solubility in amphiphilic di-block copolymer micelles: the role of polymer-drug compatibility. *Pharmazie* **2007**, *62*, 499−504.

(9) Breitkreutz, J. Prediction of intestinal drug absorption properties by three-dimensional solubility parameters. *Pharm. Res.* **1998**, *15*, 1370−1375.

(10) Ho, D. L.; Glinka, C. J. Effects of solvent solubility parameters on organoclay dispersions. *Chem. Mater.* **2003**, *15*, 1309−1312.

(11) Li, F. H.; Bao, Y.; Chai, J.; Zhang, Q. X.; Han, D. X.; Niu, L. Synthesis and Application of Widely Soluble Graphene Sheets. *Langmuir* **2010**, *26*, 12314−12320.

(12) Hansen, C. M.; Smith, A. L. Using Hansen solubility parameters to correlate solubility of C-60 fullerene in organic solvents and in polymers. *Carbon* **2004**, *42*, 1591−1597.

(13) Rostami, M.; Mohseni, M.; Ranjbar, Z. Investigating the effect of pH on the surface chemistry of an amino silane treated nano silica. *Pigm. Resin Technol.* **2011**, *40*, 363−373.

(14) Schreuder, M. A.; Gosnell, J. D.; Smith, N. J.; Warnement, M. R.; Weiss, S. M.; Rosenthal, S. J. Encapsulated white-light CdSe nanocrystals as nanophosphors for solid-state lighting. *J. Mater. Chem.* **2008**, *18*, 970−975.

(15) Wieneke, J. U.; Kommoss, B.; Gaer, O.; Prykhodko, I.; Ulbricht, M. Systematic Investigation of Dispersions of Unmodified Inorganic Nanoparticles in Organic Solvents with Focus on the Hansen Solubility Parameters. *Ind. Eng. Chem. Res.* **2012**, *51*, 327−334.

(16) Cordes, D. B.; Lickiss, P. D.; Rataboul, F. Recent Developments in the Chemistry of Cubic Polyhedral Oligosilsesquioxanes. *Chem. Rev.* **2010**, *110*, 2081−2173.

(17) Ghanbari, H.; Cousins, B. G.; Seifalian, A. M. A Nanocage for Nanomedicine: Polyhedral Oligomeric Silsesquioxane (POSS). *Macromol. Rapid Commun.* **2011**, *32*, 1032−1046.

(18) Phillips, S. H.; Haddad, T. S.; Tomczak, S. J. Developments in nanoscience: polyhedral silsesquioxane (POSS)-polymers oligomeric. *Curr. Opin. Solid State Mater. Sci.* **2004**, *8*, 21−29.

(19) Hartmann-Thompson, C. *Applications of Polyhedral Oligomeric Silsesquioxanes*; Springer: New York, 2011.

(20) Pakjamsai, C.; Kawakami, Y. Study on effective synthesis and properties of ortho-alkyl-substituted phenyl octasilsesquioxane. *Des. Monomers Polym.* **2005**, *8*, 423−435.

(21) Moore, B. M.; Ramirez, S. M.; Yandek, G. R.; Haddad, T. S.; Mabry, J. M. Asymmetric aryl polyhedral oligomeric silsesquioxanes (ArPOSS) with enhanced solubility. *J. Organomet. Chem.* **2011**, *696*, 2676−2680.

(22) Hao, N.; Boehning, M.; Schoenhals, A. Dielectric properties of nanocomposites based on polystyrene and polyhedral oligomeric phenethyl-silsesquioxanes. *Macromolecules* **2007**, *40*, 9672−9679.

(23) Iwamura, T.; Adachi, K.; Sakaguchi, M.; Chujo, Y. Synthesis of organic-inorganic polymer hybrids from poly(vinyl chloride) and polyhedral oligomeric silsesquioxane via CH/pi interaction. *Prog. Org. Coat.* **2009**, *64*, 124−127.
(24) Misra, R.; Fu, B. X.; Plagge, A.; Morgan, S. E. POSS-Nylon 6 Nanocomposites: Influence of POSS Structure on Surface and Bulk Properties. *J. Polym. Sci., Part B: Polym. Phys.* **2009**, *47*, 1088−1102.
(25) Jones, P. J.; Cook, R. D.; McWright, C. N.; Nalty, R. J.; Choudhary, V.; Morgan, S. E. Polyhedral Oligomeric Silsesquioxane-Polyphenylsulfone Nanocomposites: Investigation of the Melt-Flow Enhancement, Thermal Behavior, and Mechanical Properties. *J. Appl. Polym. Sci.* **2011**, *121*, 2945−2956.
(26) Cook, R. D.; Wei, Y. H.; Misra, R.; Morgan, S. E. Determination of polyhedral oligomeric silsesquioxane (POSS) and nylon solubility parameters for predicting dispersion in polymer composites. *Abstr. Pap. Am. Chem. Soc.* **2010**, *240*.
(27) Lim, S. K.; Hong, E. P.; Song, Y. H.; Choi, H. J.; Chin, I. J. Thermodynamic interaction and mechanical characteristics of Nylon 6 and polyhedral oligomeric silsesquioxane nanohybrids. *J. Mater. Sci.* **2012**, *47*, 308−314.
(28) Lim, S. K.; Hong, E. P.; Choi, H. J.; Chin, I. J. Polyhedral oligomeric silsesquioxane and polyethylene nanocomposites and their physical characteristics. *J. Ind. Eng. Chem.* **2010**, *16*, 189−192.
(29) Dintcheva, N. T.; Morici, E.; Arrigo, R.; La Mantia, F. P.; Malatesta, V.; Schwab, J. J. Structure-properties relationships of polyhedral oligomeric silsesquioxane (POSS) filled PS nanocomposites. *eXPRESS Polym. Lett.* **2012**, *6* (7), 561−571.
(30) Milliman, H. W.; Boris, D.; Schiraldi, D. A. Experimental Determination of Hansen Solubility Parameters for Select POSS and Polymer Compounds as a Guide to POSS-Polymer Interaction Potentials. *Macromolecules* **2012**, *45*, 1931−1936.
(31) Barra, J.; Pena, M. A.; Bustamante, P. Proposition of group molar constants for sodium to calculate the partial solubility parameters of sodium salts using the van Krevelen group contribution method. *Eur. J. Pharm. Sci.* **2000**, *10*, 153−161.
(32) Bustamante, P.; Pena, M. A.; Barra, J. The modified extended Hansen method to determine partial solubility parameters of drugs containing a single hydrogen bonding group and their sodium derivatives: benzoic acid/Na and ibuprofen/Na. *Int. J. Pharm.* **2000**, *194*, 117−124.
(33) Arita, T.; Moriya, K.; Yoshimura, T.; Minami, K.; Naka, T.; Adschiri, T. Dispersion of Phosphonic Acids Surface-Modified Titania Nanocrystals in Various Organic Solvents. *Ind. Eng. Chem. Res.* **2010**, *49*, 9815−9821.
(34) Chen, H. J.; Wang, L.; Chiu, W. Y. Chelation and solvent effect on the preparation of titania colloids. *Mater. Chem. Phys.* **2007**, *101*, 12−19.
(35) Lafaurie, A.; Azema, N.; Ferry, L.; Lopez-Cuesta, J. M. Stability parameters for mineral suspensions: Improving the dispersion of fillers in thermoplastics. *Powder Technol.* **2009**, *192*, 92−98.
(36) Shibata, J.; Fujii, K.; Horai, K.; Yamamoto, H. Dispersion and flocculation behavior of metal oxide powders in organic solvent. *Kag. Kog. Ronbunshu* **2001**, *27*, 497−501.
(37) Shibata, J.; Fujii, K.; Yamamoto, H. Dispersion and flocculation behavior of rare earth oxide powders in organic solvent. *Kag. Kog. Ronbunshu* **2002**, *28*, 641−646.
(38) Klingenfus, J.; Palmas, P. Weak molecular associations investigated by (1)H-NMR spectroscopy on a neat organosiloxane-solvent mixture. *Phys. Chem. Chem. Phys.* **2011**, *13*, 10661−10669.
(39) Schierholz, J. M. Physico-chemical properties of a rifampicin-releasing polydimethylsiloxane shunt. *Biomaterials* **1997**, *18*, 635−641.
(40) Zhou, H. L.; Su, Y.; Chen, X. R.; Wan, Y. H. Separation of acetone, butanol and ethanol (ABE) from dilute aqueous solutions by silicalite-1/PDMS hybrid pervaporation membranes. *Sep. Purif. Technol.* **2011**, *79*, 375−384.
(41) Orme, C. J.; Klaehn, J. R.; Harrup, M. K.; Lash, R. P.; Stewart, F. F. Characterization of 2-(2-methoxyethoxy)ethanol-substituted phosphazene polymers using pervaporation, solubility parameters, and sorption studies. *J. Appl. Polym. Sci.* **2005**, *97*, 939−945.
(42) Cataldo, F. On the Solubility Parameter of C60 and Higher Fullerenes. *Fullerenes, Nanotubes, Carbon Nanostruct.* **2009**, *17*, 79−84.
(43) Acevedo, S.; Castro, A.; Vasquez, E.; Marcano, F.; Ranaudo, M. A. Investigation of Physical Chemistry Properties of Asphaltenes Using Solubility Parameters of Asphaltenes and Their Fractions A1 and A2. *Energy Fuels* **2010**, *24*, 5921−5933.
(44) Aray, Y.; Hernandez-Bravo, R.; Parra, J. G.; Rodriguez, J.; Coll, D. S. Exploring the Structure-Solubility Relationship of Asphaltene Models in Toluene, Heptane, and Amphiphiles Using a Molecular Dynamic Atomistic Methodology. *J. Phys. Chem. A* **2011**, *115*, 11495−11507.
(45) Mutelet, F.; Ekulu, G.; Solimando, R.; Rogalski, M. Solubility parameters of crude oils and asphaltenes. *Energy Fuels* **2004**, *18*, 667−673.
(46) Nikooyeh, K.; Shaw, J. M. On the Applicability of the Regular Solution Theory to Asphaltene plus Diluent Mixtures. *Energy Fuels* **2012**, *26*, 576−585.
(47) Redelius, P. Bitumen solubility model using Hansen solubility parameter. *Energy Fuels* **2004**, *18*, 1087−1092.
(48) Wang, T.; Zhang, Y. Z. Methods for Determining the Solubility Parameter of Bitumen. *J. Test. Eval.* **2010**, *38*, 383−389.
(49) Hao, N.; Bohning, M.; Schonhals, A. CO(2) Gas Transport Properties of Nanocomposites Based on Polyhedral Oligomeric Phenethyl-Silsesquioxanes and Poly(bisphenol A carbonate). *Macromolecules* **2010**, *43*, 9417−9425.
(50) Voronkov, M. G.; Kovrigin, V. M.; Lavrent'ev, V. I.; Moralev, V. M. Reaction of pervinyloctasilsesquioxane with benzene in the presence of aluminum trichloride. Perphenethyloctasilsesquioxane. *Dokl. Akad. Nauk SSSR* **1985**, *281* (6).
(51) Sanchez-Soto, M.; Schiraldi, D. A.; Illescas, S. Study of the morphology and properties of melt-mixed polycarbonate-POSS nanocomposites. *Eur. Polym. J.* **2009**, *45*, 341−352.
(52) Hosaka, N.; Otsuka, H.; Hino, M.; Takahara, A. Control of dispersion state of silsesquioxane nanofillers for stabilization of polystyrene thin films. *Langmuir* **2008**, *24*, 5766−5772.
(53) Hao, N.; Bohning, M.; Goering, H.; Schonhals, A. Nanocomposites of polyhedral oligomeric phenethylsilsesquioxanes and poly(bisphenol A carbonate) as investigated by dielectric spectroscopy. *Macromolecules* **2007**, *40*, 2955−2964.
(54) Blanski, R. L.; Phillips, S. H.; Chaffee, K.; Lichtenhan, J.; Lee, A.; Geng, H. P. Preparation and properties of organic-inorganic hybrid materials by blending polyhedral oligosilsesquioxanes into organic polymers. *Polym. Prepr.* **2000**, *41*, 585−586.
(55) Blanski, R. L.; Phillips, S. H.; Chaffee, K.; Lichtenhan, J.; Lee, A.; Geng, H. P. The Synthesis of Hybrid Materials by the Blending of Polyhedral Oligosilsesquioxanes into Organic Polymers. *Mater. Res. Soc. Symp. Proc.* **2000**, *628*, CC6.27.1−CC6.27.6.
(56) Feher, F. J.; Soulivong, D.; Eklund, A. G.; Wyndham, K. D. Cross-metathesis of alkenes with vinyl-substituted silsesquioxanes and spherosilicates: A new method for synthesizing highly-functionalized Si/O frameworks. *Chem. Commun.* **1997**, 1185−1186.
(57) Chhatre, S. S.; Guardado, J. O.; Moore, B. M.; Haddad, T. S.; Mabry, J. M.; McKinley, G. H.; Cohen, R. E. Fluoroalkylated Silicon-Containing Surfaces-Estimation of Solid-Surface Energy. *ACS Appl. Mater. Interfaces* **2010**, *2*, 3544−3554.
(58) Mabry, J. M.; Vij, A.; Iacono, S. T.; Viers, B. D. Fluorinated polyhedral oligomeric silsesquioxanes (F-POSS). *Angew. Chem., Int. Ed.* **2008**, *47*, 4137−4140.
(59) Tuteja, A.; Choi, W.; Ma, M. L.; Mabry, J. M.; Mazzella, S. A.; Rutledge, G. C.; McKinley, G. H.; Cohen, R. E. Designing superoleophobic surfaces. *Science* **2007**, *318*, 1618−1622.
(60) Belmares, M.; Blanco, M.; Goddard, W. A.; Ross, R. B.; Caldwell, G.; Chou, S. H.; Pham, J.; Olofson, P. M.; Thomas, C. Hildebrand and Hansen solubility parameters from molecular dynamics with applications to electronic nose polymer sensors. *J. Comput. Chem.* **2004**, *25*, 1814−1826.
(61) Choi, P.; Kavassalis, T. A.; Rudin, A. Estimation of Hansen Solubility Parameters for (Hydroxyethyl)-Cellulose and

(Hydroxypropyl)Cellulose through Molecular Simulation. *Ind. Eng. Chem. Res.* **1994**, *33*, 3154−3159.
(62) Jarvas, G.; Quellet, C.; Dallos, A. Estimation of Hansen solubility parameters using multivariate nonlinear QSPR modeling with COSMO screening charge density moments. *Fluid Phase Equilib.* **2011**, *309*, 8−14.
(63) Tantishaiyakul, V.; Worakul, N.; Wongpoowarak, W. Prediction of solubility parameters using partial least square regression. *Int. J. Pharm.* **2006**, *325*, 8−14.
(64) Zeng, F. L.; Sun, Y.; Zhou, Y.; Li, Q. K. Molecular simulations of the miscibility in binary mixtures of PVDF and POSS compounds. *Modell. Simul. Mater. Sci. Eng.* **2009**, *17* (7).
(65) Zeng, Z. Y.; Xu, Y. Y.; Li, Y. W. Calculation of Solubility Parameter Using Perturbed-Chain SAFT and Cubic-Plus-Association Equations of State. *Ind. Eng. Chem. Res.* **2008**, *47*, 9663−9669.
(66) Stefanis, E.; Tsivintzelis, I.; Panayiotou, C. The partial solubility parameters: An equation-of-state approach. *Fluid Phase Equilib.* **2006**, *240*, 144−154.
(67) Constantinou, L.; Gani, R.; Oconnell, J. P. Estimation of the acentric factor and the liquid molar volume at 298-K using a new group-contribution method. *Fluid Phase Equilib.* **1995**, *103*, 11−22.
(68) Stefanis, E.; Panayiotou, C. Prediction of Hansen solubility parameters with a new group-contribution method. *Int. J. Thermophys.* **2008**, *29*, 568−585.
(69) Lavrent'ev, V. I. Per(gamma-trifluoropropyl)octasilsesquioxane. *Russ. J. Gen. Chem.* **2004**, *74*, 1188−1193.
(70) Iacono, S. T.; Vij, A.; Grabow, W.; Smith, D. W.; Mabry, J. M. Facile synthesis of hydrophobic fluoroalkyl functionalized silsesquioxane nanostructures. *Chem. Commun.* **2007**, 4992−4994.